

METHODS & TECHNIQUES

Characterizing the hypoxic performance of a fish using a new metric: P_{AAS-50}

Yangfan Zhang^{1,2,*}, Daniel W. Montgomery¹, Connor F. White², Jeffrey G. Richards¹, Colin J. Brauner¹ and Anthony P. Farrell¹

ABSTRACT

The hypoxic constraint on peak oxygen uptake ($\dot{M}_{O_2,peak}$) was characterized in rainbow trout over a range of ambient oxygen tensions with different testing protocols and statistical models. The best-fit model was selected using both statistical criteria (R^2 and AIC) and the model's prediction of three anchor points for hypoxic performance: critical P_{O_2} (P_{crit}), maximum \dot{M}_{O_2} and a new metric, the minimum P_{O_2} that supports 50% of absolute aerobic scope (P_{AAS-50}). The best-fitting model was curvilinear using five strategically selected P_{O_2} values. This model predicted P_{AAS-50} as 70 mmHg (coefficient of variation, CV=9%) for rainbow trout. Thus, while a five-point hypoxic performance curve can characterize the limiting effects of hypoxia in fish, as envisaged by Fry over 75 years ago, P_{AAS-50} is a promising metric to compare hypoxic constraints on performance in a standardized manner both within and across fish species.

KEY WORDS: Respirometry, Hypoxia, Maximum oxygen uptake, Aerobic scope, Metabolic rate, Exercise

INTRODUCTION

How an animal's metabolic rate interacts with its ambient environment has long fascinated biologists. For example, characterizing how ambient oxygen constrains whole-organism oxygen uptake (\dot{M}_{O_2}) has a long history (Warburg, 1914; Hyman, 1929; Tang, 1933), whether the interest lies with birds flying above the Tibetan Plateau (Black and Tenney, 1980; Lague et al., 2017), with mammals living at alpine regions (Terrados et al., 1988; Ivy and Scott, 2017), or with fishes exploiting oceanic oxygen minimum zones (Douglas et al., 1976) and oxygen-depleted lakes (Lefevre et al., 2014). While severely depleted levels of ambient oxygen ultimately constrain an animal's basal or standard metabolic rate (SMR), a less severe level of hypoxia constrains its maximum \dot{M}_{O_2} ($\dot{M}_{O_2,max}$). For clarity, we define $\dot{M}_{O_2,max}$ as the highest attainable \dot{M}_{O_2} measured under normoxic conditions and use the term peak \dot{M}_{O_2} ($\dot{M}_{O_2,peak}$) as the highest attainable \dot{M}_{O_2} measured under all hypoxic conditions. Knowing the exact nature of hypoxia constraint has important physiological and ecological implications because $\dot{M}_{O_2,peak}$ sets the ceiling for all aerobic activity above SMR. However, measuring $\dot{M}_{O_2,peak}$ during progressive hypoxia to assess how hypoxia constrains peak aerobic performance is far more

technically challenging than measuring routine \dot{M}_{O_2} ($\dot{M}_{O_2,routine}$). As such, despite its obvious importance, relatively few studies have characterized how hypoxia constrains peak aerobic performance in fish.

In fish, the limiting effect of declining ambient oxygen levels on the maximum exercise-induced \dot{M}_{O_2} (by critical swim or exhaustive chase protocols), which we collectively term hypoxic performance models, can take three general forms (Fig. 1A; Fry and Hart, 1948; Neill et al., 1994; Claireaux and Lagardère, 1999; Chabot and Claireaux, 2008; Zhang et al., 2021). For all these models, one anchor point is $\dot{M}_{O_2,max}$ and the other is the critical ambient partial pressure of oxygen (P_{crit} , mmHg). SMR, $\dot{M}_{O_2,routine}$ and $\dot{M}_{O_2,peak}$ of a fish should all converge at P_{crit} (i.e. zero absolute aerobic scope, AAS; Fry and Hart, 1948). In between these two anchor points are three general models. The simplest is a linear model where $\dot{M}_{O_2,peak}$ conforms with the partial pressure of oxygen (P_{O_2}) (model I). A partial oxyregulation model (model II) is where $\dot{M}_{O_2,peak}$ under modest hypoxic conditions is independent of ambient oxygen and identical to $\dot{M}_{O_2,max}$ (Fig. 1A; Fig. S1), followed by a linear phase of oxyconforming. Model III has two linear phases of oxyconforming. Variations on models II and III occur when the $\dot{M}_{O_2,peak}$ dependence on P_{O_2} is curvilinear (models IIa and IIIa) rather than linear. A curvilinear model requires more data points to adequately model the hypoxic performance curve relative to a linear model, where a curvilinear model sometimes uses a third value as a reference point. Indeed, curvilinear models could use the midway point between SMR and $\dot{M}_{O_2,max}$, the minimum P_{O_2} that would support 50% of AAS (P_{AAS-50}), as a reference point. Regardless of the model, $\dot{M}_{O_2,peak}$ needs to be repeatedly measured over a range of P_{O_2} values. It is this challenge that we address here.

Improvements in the techniques and protocols used in aquatic respirometry have done much to pave the way for repeatedly exercising individual fish at multiple levels of hypoxia, which is a requirement for generating a hypoxic performance model. In particular, chasing a fish inside rather than outside a static respirometer allows \dot{M}_{O_2} to be closely monitored during and immediately following exercise, ensuring that $\dot{M}_{O_2,peak}$ is not missed (Zhang and Gilbert, 2017; Zhang et al., 2020). Analysis of the decline in P_{O_2} due to fish respiration has also improved. For example, $\dot{M}_{O_2,peak}$ is estimated more accurately by minimizing the duration of the sampling window for each \dot{M}_{O_2} determination and using an iterative algorithm to specifically identify $\dot{M}_{O_2,peak}$ (Zhang et al., 2019; Prinzing et al., 2021).

In the present study, we had three objectives. The first was to determine the best statistical model to apply to $\dot{M}_{O_2,peak}$ data. The second was to define the minimum number of P_{O_2} values needed for accurate modelling and prediction of P_{AAS-50} . While minimizing the number of P_{O_2} values reduces the number of separate exercise bouts per fish, the potential confounding effect of cumulative stress, which could reduce $\dot{M}_{O_2,peak}$, is decreased but not completely

¹Department of Zoology and Faculty of Land and Food Systems, University of British Columbia, Vancouver, BC, Canada, V6T 1Z4. ²Department of Organismic and Evolutionary Biology, Harvard University, 26 Oxford Street, Cambridge, MA 02138, USA.

*Author for correspondence (yangfan_zhang@fas.harvard.edu)

 Y.Z., 0000-0001-5625-6409

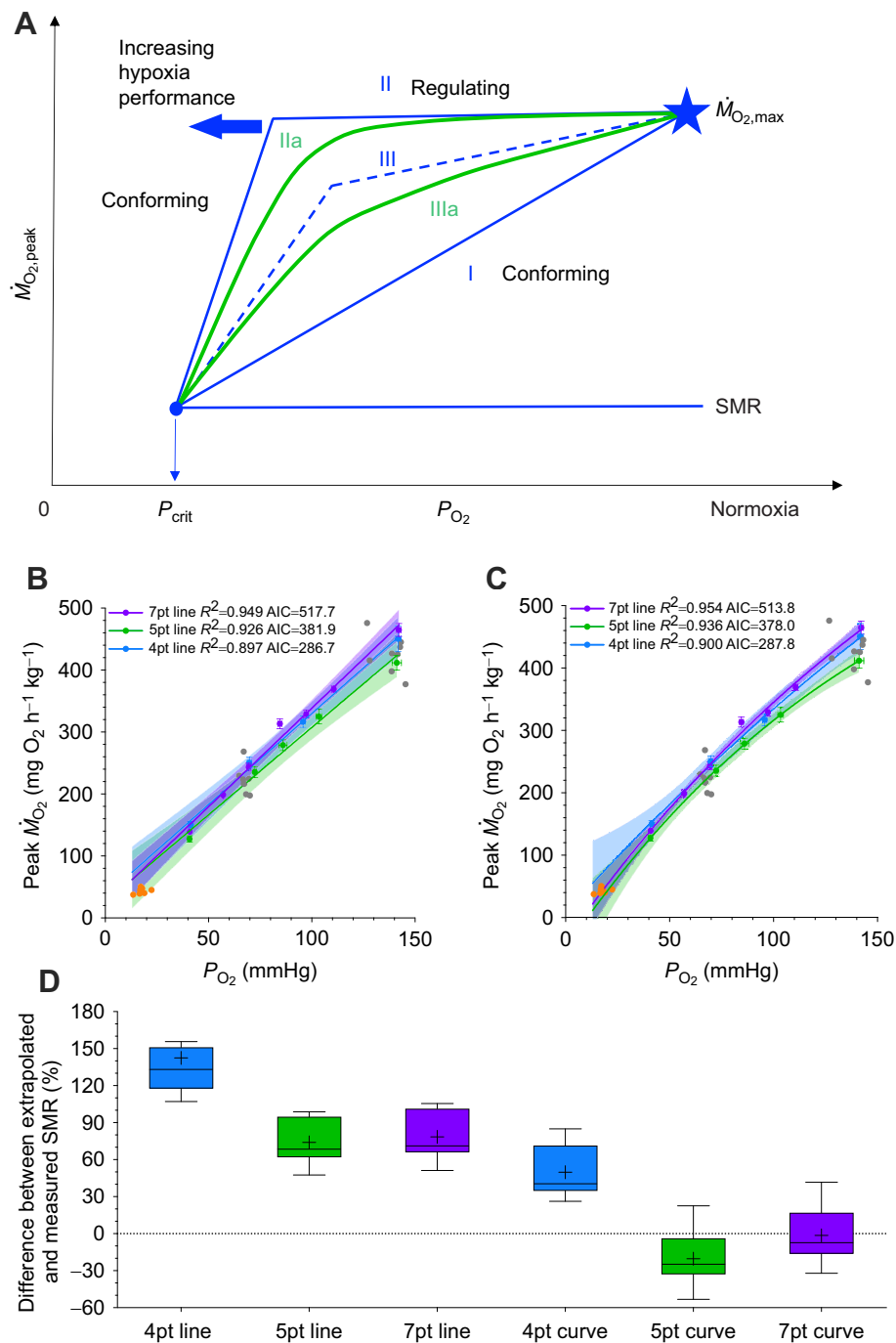


Fig. 1. Theoretical hypoxic performance models. (A) Three types of models are presented for the relationship between exercise-induced peak oxygen uptake ($\dot{M}_{O_2,peak}$) and ambient oxygen partial pressure (P_{O_2}). The maximum oxygen uptake ($\dot{M}_{O_2,max}$) and standard metabolic rate (SMR) are the reference framework. The details of the models are given in the Introduction and in Fig. S1. (B,C) $\dot{M}_{O_2,peak}$ values (each point is the mean \pm s.e.m.) for rainbow trout (*Oncorhynchus mykiss*) with independent datasets for the four-point (4pt, $n=7$), five-point (5pt, $n=8$) and seven-point (7pt, $n=8$) testing protocols. These data were statistically modelled (line indicates mean and shading shows the 95% confidence interval, CI) with either a linear regression model (B) or an asymptotic model (curvilinear fit) (C) (see table S2 in figshare <https://doi.org/10.6084/m9.figshare.19658568.v3>, for all equations). As reference points, independent control measurements of individual P_{crit} (critical ambient partial pressure of oxygen) and SMR values are in orange and independently measured values for individual $\dot{M}_{O_2,max}$ and $\dot{M}_{O_2,peak}$ in naive fish are in grey. (D) Percentage difference of the deviation between the measured $\dot{M}_{O_2,min}$ in the control fish (mean of the orange symbols) and estimated values obtained by extrapolating both the linear (B) and curvilinear (C) hypoxic performance models for the three different datasets (bar indicates 25–75 percentile, whiskers show minimum–maximum, line indicates median, crosses indicate mean).

eliminated. Therefore, our third objective was to use a control group of fish to independently measure $\dot{M}_{O_2,max}$ and $\dot{M}_{O_2,peak}$ at only one level of hypoxia, near the P_{AAS-50} , to determine the degree to which cumulative stress may affect P_{AAS-50} . By satisfying these objectives, we arrived at a recommendation for a testing protocol that reliably quantified the hypoxic performance of individual rainbow trout (*Oncorhynchus mykiss*). This testing protocol advances our ability to capture inter-individual variation relative to an earlier methodology that characterized hypoxic performance in a group of European sea bass (*Dicentrarchus labrax*) by using different individuals at multiple levels of hypoxia (Claireaux and Lagardère, 1999). Moreover, we generated a reliable estimate of P_{AAS-50} , which has the potential to be a standardized metric to compare hypoxic performance within and across fish species.

MATERIALS AND METHODS

Experimental animals

The experiments were performed on a hatchery-reared, Fraser Valley strain of rainbow trout, *Oncorhynchus mykiss* (Walbaum 1792) ($n=23$ fish, body mass: 126.4 ± 4.8 g) (Fraser Valley Trout Hatchery, Abbotsford, BC, Canada; Freshwater Fisheries Society of British Columbia). They were held in 200 l circular tanks containing dechlorinated Vancouver tap water in the Department of Zoology, University of British Columbia (UBC) Aquatics Facility for over 1.5 years prior to experimentation. Monitoring of water temperature (11°C for at least 3 months before experimentation started) and fish feeding (a maintenance ration, 1% body mass, of commercial trout pellets; Skretting Canada Inc., Vancouver, BC, Canada) were performed daily. Animal holding and experimental

procedures were approved by The UBC Animal Care Committee (A18-0340).

Respirometry apparatus

The hypoxic performance trials were conducted on individual fish (fasted for 48 h) placed into one of four replicate 4.1 l Loligo-type, static respirometers (water volume to fish mass ratio ~33:1; Loligo Systems, Tjele, Denmark). Fish were habituated to normoxic conditions with the respirometer in a water flush mode for at least 30 min before the first chase (see below) to ensure that fish at least repaid the high-energy phosphate and oxygen stores that might be partially consumed during handling (Zhang et al., 2018). The respirometers were submerged in a water table (2.4×0.8×0.4 m) filled with fully aerated freshwater, which accommodated all four respirometers and allowed simultaneous measurements on four individuals. A water temperature regulator (Ecoplus ¼ HP chiller, Vancouver, BC, USA) maintained the temperature of the water table at 11°C and circulated the contents of the water table. The entire respirometry system was located inside a thermally regulated (11°C) environmental chamber. The water volume of the entire system was replaced in between trials. Every 5 days, the entire respirometry system was disinfected with Virkon Aquatic (10 g l⁻¹; Syndel, Nanaimo, BC, Canada), rinsed thoroughly, and the water in the respirometers and water table replaced.

The water from the water table was intermittently circulated through each respirometer using individual, computer-controlled (AquaResp v.3, Aquaresp.com) flush pumps (Universal 3400, EHEIM, Deizisau, Germany). Flush pumps were stopped at the beginning of each 600 s \dot{M}_{O_2} monitoring period (AquaResp v.3, Aquaresp.com), which was followed by 30 s flush and 40 s equilibration periods. Each respirometer also had a recirculation loop which contained a dedicated external pump (Universal 600, EHEIM) and an optical oxygen probe (Robust Oxygen Probe OXROB10) to continuously record the P_{O_2} (mmHg) of ambient water inside the respirometer (recording frequency ~1 Hz, response time <15 s, PyroScience GmbH, Aachen, Germany). Oxygen probes were calibrated to 0 mmHg (0 kPa, water saturated with sodium sulphite and bubbled with nitrogen gas) and fully aerated water (157 mmHg=20.9 kPa). The background \dot{M}_{O_2} in each respirometer was measured for 25 min after each trial had been completed. On the few occasions where background exceeded 1% of $\dot{M}_{O_2, routine}$, a correction was applied to the \dot{M}_{O_2} measurement.

Each respirometer was equipped with a chasing device (a soft piece of 25 cm cable tie attached to a 20 cm metal stem bent at a right angle and inserted through a 1.5 cm diameter sealed port located mid-way along the top of the respirometer; Zhang et al., 2020), which when repeatedly turned from the outside would agitate the fish to perform C-start turns until it fatigued.

Assessment of hypoxic performance

Modelling hypoxic performance above the P_{crit} (17.6 mmHg or 2.3 kPa; see below) required a preliminary trial ($n=3$ fish) to strategically select the ambient P_{O_2} test range to bracket the anticipated P_{AAS-50} , much like acute toxicity testing brackets median lethal concentrations. Based on these preliminary data, three testing protocols (four-point, five-point and seven-point P_{O_2} levels) were designed ($n=7-8$ fish for each protocol): the four-point model used P_{O_2} levels of 142, 96, 70 and 41 mmHg (18.9, 12.8, 9.3 and 5.5 kPa), the five-point model used P_{O_2} levels of 141, 103, 86, 72 and 40 mmHg (18.8, 13.7, 11.5, 9.6 and 5.3 kPa) and the 7-point model used P_{O_2} levels of 142, 110, 97, 84, 69, 57 and 41 mmHg (18.9, 14.7, 12.9, 11.2, 9.2, 7.6 and 5.5 kPa) (all values are the mean

value for the mid-point of the ambient P_{O_2} while the respirometer was closed). Each testing protocol involved a stepwise deoxygenation of the respirometers with an $\dot{M}_{O_2, peak}$ determination (described below) at each P_{O_2} level. Thus, the three testing protocols all started with an $\dot{M}_{O_2, peak}$ at normoxia for each fish and then examined 3, 4 or 6 levels of hypoxia for that fish.

$\dot{M}_{O_2, peak}$ was measured at each of these P_{O_2} levels by turning off the flush pumps and sealing the respirometer. Each fish was then individually exercised to fatigue by rapidly turning the chasing device for 5 min, after which it was left undisturbed for 5 min to

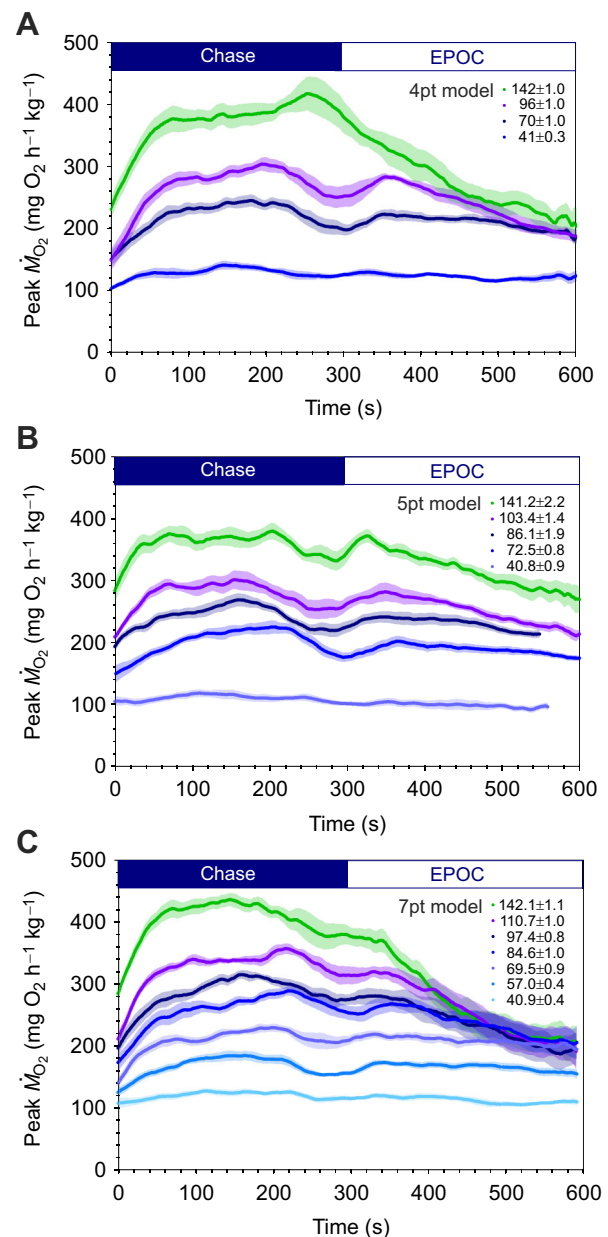


Fig. 2. Continuous $\dot{M}_{O_2, peak}$ of rainbow trout (*O. mykiss*) during chasing and recovery periods, and as a function of ambient P_{O_2} . The key provides details on the mean (\pm s.e.m.) P_{O_2} (mmHg) to illustrate both the sustained nature of $\dot{M}_{O_2, peak}$ while chasing a rainbow trout and the constraint placed upon $\dot{M}_{O_2, peak}$ by decreasing P_{O_2} . At progressively lower P_{O_2} values and with suitable recovery periods in between, $\dot{M}_{O_2, peak}$ was monitored while a fish was chased inside the respirometer for 300 s and during the ensuing 300 s excess post-exercise oxygen consumption (EPOC). Each coloured line represents the mean $\dot{M}_{O_2, peak}$ at a given P_{O_2} and shading represents s.e.m.

capture the initial portion of the excess post-exercise oxygen consumption (EPOC; Fig. 2), i.e. a closed monitoring cycle of 10 min. Subsequent off-line analysis captured the highest \dot{M}_{O_2} values during this 10 min \dot{M}_{O_2} monitoring period, and $\dot{M}_{O_{2,peak}}$ was assigned to the highest of these values (see below and representative individual traces in Fig. S1), and the associated P_{O_2} was defined as peak P_{O_2} ($P_{O_{2,peak}}$; see calculation in ‘Data analysis’, ‘ \dot{M}_{O_2} , $\dot{M}_{O_{2,peak}}$ and SMR analysis’, below; and values in Figs 1 and 3). At the end of each 10 min \dot{M}_{O_2} monitoring period, the respirometer flush pumps were turned on to introduce hypoxic water into the respirometer and gradually achieve one of the predetermined P_{O_2} levels outlined above using a 4 min cycle of a 30 s flush period, a 40 s equilibration period and a 170 s \dot{M}_{O_2} monitoring period. Hypoxic water was generated using a custom-built, 10 l gas equilibration column situated upstream of the water table (it received the normoxic water at the top and nitrogen gas was injected at the bottom) and reduced the water P_{O_2} of the entire respirometry system. This exercise protocol was repeated at each P_{O_2} test level. Thus, each 10 min period when a fish was exercised and began recovery was followed by a 20 min recovery period during which \dot{M}_{O_2} was monitored on-line (data not presented). This same protocol was followed for each P_{O_2} test

level except the final one (39–42 mmHg or 5.2–5.6 kPa), which required a slightly longer degassing period (~30 min) to reach the desired ambient P_{O_2} . At the end of the trial, the fish were removed from their respirometers and returned to three holding tanks where the four-, five- and seven-point test groups were kept separated. After a 10-day recovery, the same fish from the five-point or seven-point test groups were re-tested to check the repeatability of the five-point and seven-point models. The four-point protocol was not repeated after it produced an inferior hypoxic performance curve (see Results). Additional details concerning the respirometry system and the testing protocols are available from figshare (<https://doi.org/10.6084/m9.figshare.19658568.v3>, table S1).

Independent measurement of SMR, P_{crit} and $\dot{M}_{O_{2,peak}}$ in normoxia and near P_{AAS-50}

SMR, $\dot{M}_{O_{2,peak}}$ in normoxia and $\dot{M}_{O_{2,peak}}$ at P_{AAS-50} were independently measured on a group of 8 naive fish using the same test apparatus, measurement protocols and chasing protocols as described above. However, once $\dot{M}_{O_{2,peak}}$ was measured in normoxia, the fish were left undisturbed in the respirometer, which was continuously flushed with normoxic water for a 2 day quiescent period during which $\dot{M}_{O_{2,routine}}$ was continuously measured and SMR

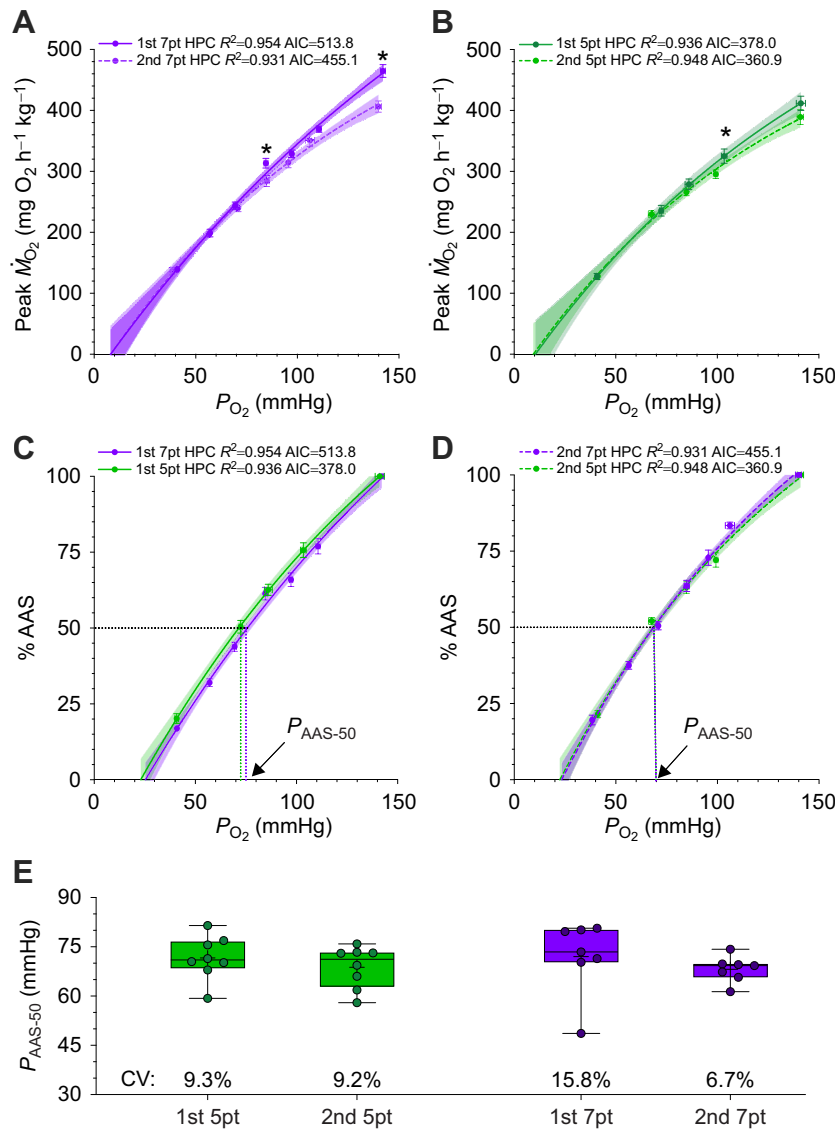


Fig. 3. The reproducibility of the hypoxic performance curve. (A,B) The same rainbow trout (*O. mykiss*) were measured for either seven-point (A) or five-point (B) hypoxic performance curve (HPC). Peak oxygen uptake ($\dot{M}_{O_{2,peak}}$) and ambient oxygen partial pressure (P_{O_2}) were fitted by asymptotic association equations (line indicates mean and shading shows the 95% CI). The reproducibility was tested on the difference of $\dot{M}_{O_{2,peak}}$ values at the similar P_{O_2} range (asterisk denotes $\alpha < 0.05$ by paired *t*-tests) and the three parameters (i.e. asymptote, rate constant for a hyperbolic increase, and intercept) in a non-linear mixed-effects model (see table S3 in figshare, <https://doi.org/10.6084/m9.figshare.19658568.v3>). (C,D) The $\dot{M}_{O_{2,peak}}$ values were normalized to a percentage of the absolute aerobic scope (AAS) of the same individual to derive the minimum P_{O_2} at which the fish generates 50% of its absolute aerobic scope (P_{AAS-50}) in the first (C) and the second tests (D). (E) The P_{AAS-50} values derived from each individual, summarized in bar and whisker plots (bar indicates 25–75 percentile, whiskers show minimum–maximum, line indicates median, crosses indicate mean) with the coefficient of variation (CV).

was estimated from these measurements (see below). After this quiescent period, the water was gradually deoxygenated at a similar rate (total time ~50 min) to near the P_{AAS-50} estimated from the hypoxic performance curve (around 75 mmHg=9.9 kPa), at which point another $\dot{M}_{O_2,peak}$ determination was made as described above. These estimates of $\dot{M}_{O_2,peak}$ in normoxia and at P_{AAS-50} were statistically compared with those obtained with the hypoxic performance testing protocol to examine whether cumulative exercise in hypoxia affected these estimates. SMR was statistically compared with an independent measurement of SMR from another group of eight naive fish that were never chased. These additional fish were placed into the respirometers and left undisturbed under normoxic conditions for a similar 2 day quiescent period during which $\dot{M}_{O_2,routine}$ was continuously measured to determine SMR. After this quiescent period, a well-established hypoxia challenge test (Claireaux et al., 2013) was performed to provide an estimate of P_{crit} (Claireaux and Chabot, 2016).

Data analysis

\dot{M}_{O_2} , $\dot{M}_{O_2,peak}$ and SMR analysis

\dot{M}_{O_2} values ($\text{mg O}_2 \text{ h}^{-1} \text{ kg}^{-1}$) at each ambient water P_{O_2} level were determined with off-line analysis of the continuous measurement of the declining water P_{O_2} when the respirometer was closed during a measurement cycle. An iterative algorithm (Eqn 1) was applied (Zhang et al., 2019), one that slides a minimum sampling window duration as a rolling regression through the continuous, 10 min P_{O_2} trace. A minimum sampling window duration for a reliable \dot{M}_{O_2} determination was 100 s, based on an analysis of eight background \dot{M}_{O_2} traces (Fig. S2). $\dot{M}_{O_2,peak}$ was defined as the highest \dot{M}_{O_2} attained during a 5 min chase of fish inside the static respirometer (higher values were not obtained during EPOC; Fig. 2; Fig. S1). The $P_{O_2,peak}$ was the mid-point of the P_{O_2} slope used for this $\dot{M}_{O_2,peak}$ determination. On-line reporting of \dot{M}_{O_2} (set by AquaResp v.3 software) was only used for monitoring purposes. Rolling regression analysis:

$$\dot{M}_{O_2,peak} = \max \left\{ \left[\frac{dDO_{[n,(n+a)]}}{dt_{[n,(n+a)]}} \times (V_r - V_f) \times S_O \right] / (t \times M_f) \right\}; \quad (1)$$

sequential interval regression analysis:

$$\dot{M}_{O_2} = \left[\frac{dDO_{[i,(i+a)]}}{dt_{[i,(i+a)]}} \times (V_r - V_f) \times S_O \right] / (t \times M_f), \quad (2)$$

where dDO/dt is the change in O_2 saturation with time, V_r is the respirometer volume, V_f is the fish volume (1 g body mass=1 ml water), S_O is the water solubility of O_2 (calculated by AquaResp v.3 software) at the experimental temperature, salinity and atmospheric pressure, t is a time constant of 3600 s h^{-1} , M_f is fish mass, n is one P_{O_2} sample forward from the first P_{O_2} recorded in the sealed respirometer, a is the sampling window duration of 100 s, and i is the next P_{O_2} sample after the preceding sampling window.

SMR was estimated from ~288 \dot{M}_{O_2} calculations using Eqn 2 collected during a 2 day quiescent period in the respirometer and applying a 20th quantile algorithm (Chabot et al., 2016, 2021). P_{crit} was estimated by fitting a linear regression function of ambient water P_{O_2} to the declining \dot{M}_{O_2} (calculated using Eqn 2) during the final stages of the hypoxia challenge test. P_{crit} was assigned to the P_{O_2} by solving this regression for SMR (Claireaux and Chabot, 2016), i.e. the intersection of the regression line with SMR (Fig. 1).

Statistical modelling of hypoxic performance: $\dot{M}_{O_2,peak}$ as a function of ambient P_{O_2}

The responses of $\dot{M}_{O_2,peak}$ (y) as a function of ambient water P_{O_2} (x) were statistically modelled with both a linear regression equation (Eqn 3) and an asymptotic equation (Eqn 4) (Mueller and Seymour, 2011). The quality of these statistical fits for the four-point, five-point and seven-point datasets was assessed by least-squares regressions following Akaike information criterion (AIC) (for model parameters, see table S2 in figshare, <https://doi.org/10.6084/m9.figshare.19658568.v3>).

Linear regression equation:

$$y = a \times x + b, \quad (3)$$

where a is the slope, a rate constant for a linear increase, and b is the intercept at the y -axis.

Asymptotic equation:

$$y = \text{Asymptote}(1 - e^{-e^K(x-I)}), \quad (4)$$

where I is the intercept at the x -axis (and is expressed in the same units as x), Asymptote is a line that the curve continues to approach at infinity (and is expressed in the same units as y) and K is the rate constant.

The repeatability of the five-point and seven-point hypoxic performance models was statistically tested by comparing the 1st and 2nd determinations using a non-linear mixed-effects model (Eqn 5) (lmerTest package in R v.4.1.1).

Reproducibility test for asymptotic equation:

$$y = (\text{Asymptote} + a)(1 - e^{-e^{K+b}(x-I+c)}), \quad (5)$$

where a , b and c are the respective modifiers for the Asymptote, the rate constant for a hyperbolic increase (K) and the intercept (I) for the 2nd hypoxic performance test (Eqn 5). If the modifiers reached statistical significance ($\alpha < 0.05$), the two asymptotic equations were deemed different.

P_{AAS-50} was estimated by normalizing individual $\dot{M}_{O_2,peak}$ values to a percentage of their individual AAS ($AAS = \dot{M}_{O_2,max} - SMR$) and interpolating P_{AAS-50} as the minimum P_{O_2} supporting the 50% of AAS from the best-fitted hypoxic performance model. The extrapolated SMR values were calculated based on P_{crit} using the best-fitted hypoxic performance model.

Statistical analysis

Measurements points were presented as mean \pm s.e.m. for $\dot{M}_{O_2,peak}$ and $P_{O_2,peak}$, and 95% confidence interval (CI) was provided for the hypoxic performance equations. Logarithm transformations were applied on the metrics that failed normality tests to meet the assumptions of normality of residuals, homoscedasticity of the residuals and no trend in the explanatory variables. Statistical comparisons among different individuals, and for measured and extrapolated \dot{M}_{O_2} values used one-way ANOVA with Holm-Šidák *post hoc* tests. The comparisons of the same individuals used paired t -tests. The statistical analyses were conducted in SPSS v.26 (SPSS Inc. Chicago, IL, USA). The best-fitting regression analyses were conducted using Prism v.9 (GraphPad Software, San Diego, CA, USA). Significance was assigned when $\alpha < 0.05$. Analysis of the respirometry data was performed in R v.4.1.1 software and R studio (<https://www.rstudio.com/products/team/>) using either the fishMO2 package (Claireaux and Chabot, 2016) or LabChart v.8.0 (ADInstruments, Colorado Springs, CO, USA).

RESULTS AND DISCUSSION

$\dot{M}_{O_2,peak}$ was typically reached during the chase (sometimes more than once), but rarely during the EPOC period (Fig. 2; Figs S1–S3). While \dot{M}_{O_2} typically declined exponentially when P_{O_2} was above ~ 100 mmHg, \dot{M}_{O_2} remained quite constant during EPOC below ~ 70 mmHg (Fig. 2). Thus, we confirm that chasing fish inside a respirometer provides a more reliable measurement of $\dot{M}_{O_2,peak}$ than quickly transferring an exhausted fish into a respirometer and measuring \dot{M}_{O_2} during the initial phase of EPOC (Zhang et al., 2020). Thus, a key criterion of measuring $\dot{M}_{O_2,peak}$ is that a sustained workload on an individual is a prerequisite of a sustained peak performance (Midgley et al., 2007; Copp et al., 2009). In addition, we confirmed the normoxic anchor points by showing that an independently measured $\dot{M}_{O_2,peak}$ at normoxia was indistinguishable from that determined with the hypoxic performance protocol ($F=0.574$, $P=0.637$, power=0.662; Fig. 1; Fig. S3).

We rejected a two-segmented linear regression model for the rainbow trout and compared a linear regression model with an asymptotic model for the best statistical fit. The former is often used to evaluate the dependence of $\dot{M}_{O_2,routine}$ on P_{O_2} (Ultsch et al., 1980), while the latter models are used for hypoxic performance modelling (Mueller and Seymour, 2011). An asymptotic equation (curvilinear) modelled the hypoxic performance of rainbow trout no better than a linear regression equation based on AIC (AIC four-point: 287.8 versus 286.7, five-point: 378.0 versus 381.9, seven-point: 513.8 versus 517.7) and only marginally better based on R^2 (R^2 four-point: 0.900 versus 0.897, five-point: 0.936 versus 0.926, seven-point: 0.954 versus 0.949) (Fig. 1; see table S2 in figshare <https://doi.org/10.6084/m9.figshare.19658568.v3>). However, the curvilinear model was superior to the linear regression in terms of predicting the second anchor point of hypoxic performance, SMR; solving and extrapolating the linear models for the independently measured P_{crit} (17.6 ± 0.9 mmHg, Fig. 1B,C) consistently overestimated SMR ($76.0\text{--}90.9$ mg O_2 h^{-1} kg^{-1}) by a very large amount (74–143%) compared with the independently measured SMR value (SMR=43.9 mg O_2 h^{-1} kg^{-1} ; $F=46.85$, $P<0.0001$; Fig. 1). In contrast, extrapolation of the five- and seven-point asymptotic equations (35.1 ± 3.8 and 43.4 ± 3.8 mg O_2 h^{-1} kg^{-1} , $F=2.3$, $P=0.12$, power=0.394; Fig. 1) reliably predicted the measured SMR. Thus, using either five or seven strategically selected P_{O_2} values with an asymptotic equation generated a reliable characterization of the hypoxic performance curve for rainbow trout, one that accurately predicted SMR using a known P_{crit} . However, we rejected a four-point curvilinear model because it also overestimated SMR by 50% (SMR=65.6 mg O_2 h^{-1} kg^{-1} , $F=38.11$, $P<0.001$) despite a good statistical fit ($R^2=0.900$; AIC=287.8).

We proposed P_{AAS-50} as a potential third anchor point of a hypoxic performance curve. P_{AAS-50} interpolations were statistically indistinguishable ($t=0.10$, $P=0.92$, power=0.051) for the five-point (first test 71.6 ± 2.3 mmHg, second test 68.8 ± 2.2 mmHg) and seven-point (first test 72.1 ± 4.2 mmHg, second test 68.2 ± 1.5 mmHg) curvilinear models. Also, the interpolated $\dot{M}_{O_2,peak}$ values at P_{AAS-50} were indistinguishable from the independent measurements ($F=2.047$, $P=0.131$, power=0.466; Fig. 1; Fig. S3). Consequently, five strategically selected P_{O_2} levels are likely the minimum number of data points needed to reliably model a hypoxic performance curve and predict P_{AAS-50} . Nevertheless, further studies are needed to understand whether a curvilinear or a linear model applies to the hypoxic performance of other fish species.

The reproducibility of the five-point and seven-point hypoxic performance curve protocols was confirmed by retesting the same

individuals after a 10 day recovery period. The re-tested five-point hypoxic performance curve only manifested the slower rate of decline than the first test ($t=2.49$, $P=0.015$; see table S3 in figshare <https://doi.org/10.6084/m9.figshare.19658568.v3>; Fig. 3) whereas the re-tested seven-point hypoxic performance curve manifested a slower rate of decline (i.e. the lower tangent; $t=2.49$, $P=0.015$) and a lower asymptote ($t=2.07$, $P=0.04$) than the first test. Consequently, $\dot{M}_{O_2,peak}$ at normoxia for the re-tested five-point hypoxic performance curve was only 9% lower than that for the first test ($t=2.86$, $P=0.024$; Fig. 3) and 12% lower with the re-tested seven-point hypoxic performance curve. $\dot{M}_{O_2,peak}$ for the re-tested five-point hypoxic performance had an 8% lower $\dot{M}_{O_2,peak}$ at 85 mmHg ($t \geq 4.05$, $P \leq 0.007$) than the first test. Despite the inconsequential difference in the $\dot{M}_{O_2,peak}$ values, P_{AAS-50} values for the re-tests were indistinguishable from those of the first tests ($t=0.22$, $P=0.82$, power=0.055) (Fig. 3).

The consistent values for $\dot{M}_{O_2,peak}$ at P_{AAS-50} by independent means suggest that the cumulative stress associated with repeat chasing to fatigue did not impact this variable. This finding implies that rainbow trout exercised to fatigue for 5 min and allowed to recover for 25 min can repeat their peak performance even though the fish only partially repaid their EPOC. Indeed, exhausted salmonids take about 30 min to replenish the majority of their oxygen stores and high-energy phosphate (Wood, 1991; Scarabello et al., 1991, 1992; Zhang et al., 2018) and salmonids can repeat a critical swimming test after just a 20–40 min recovery from the fatigue experienced in the previous test while carrying some unpaid EPOC (Randall et al., 1987; Jain et al., 1997, 1998; Farrell et al., 1998, 2001; Wagner et al., 2006; Steinhausen et al., 2008). Likewise, European sea bass (*D. labrax*) repeated four constant acceleration tests with only a 5 min rest period between tests (Marras et al., 2010). Whether or not other fish species can repeatedly perform as quickly remains to be determined.

The low coefficient of variation for the P_{AAS-50} (<10% for both five-point determinations) suggests that it may be a robust and potentially valuable metric to compare hypoxic performance curves across fish species or within a species across different ambient environments. Also, it is tempting to suggest that the curvilinear nature of the rainbow trout hypoxic performance curve reflects the sigmoidal shape of the blood oxygen equilibrium curve (Weber et al., 1987). However, the P_{AAS-50} was around 70 mmHg, which is approximately twice the P_{50} of exercised rainbow trout haemoglobin (~ 35 mmHg; Rummer and Brauner, 2015). Therefore, other physiological factors must affect the positioning of the curvilinear hypoxic performance of rainbow trout.

What is clear from our data, however, is that a linear model is inaccurate over a wide range of P_{O_2} values. A linear model with the anchor points of P_{crit} and the zero intercept for \dot{M}_{O_2} and P_{O_2} has been used in a different context to describe hypoxic performance (Seibel et al., 2021). However, all our hypoxic performance curve models had non-zero intercepts (see table S2 in figshare <https://doi.org/10.6084/m9.figshare.19658568.v3>; Fig. 1B,C), suggesting that forcing the intercept through the origin lacks biological relevance, at least in trout. Moreover, such a linear model was suggested to be able to predict $\dot{M}_{O_2,max}$ (Seibel et al., 2021), presumably at normoxia. However, this extrapolation for our measured P_{crit} in rainbow trout predicted a $\dot{M}_{O_2,max}$ that was 13% lower ($t=2.73$, $P=0.009$; 357 mg O_2 h^{-1} kg^{-1}) than our measured value. While such a difference can be considered small, larger differences might be expected when such extrapolations are made for fishes with a lower P_{crit} than rainbow trout. In particular, the linear extrapolation

through the origin for the measured P_{crit} value in European sea bass (*D. labrax*) (Zhang, 2021) predicted a $\dot{M}_{O_2,max}$ that was 47% higher than that measured ($t=12.7$, $P<0.0001$). Thus, any such linear models and extrapolations should be conducted with caution.

In conclusion, the hypoxic performance curve protocol provides a respiratory phenotyping platform to compare a fish's ability to exercise under hypoxia. We recommend the five-point hypoxic performance curve as a reliable, time-efficient and reproducible methodology to functionally quantify the hypoxic performance of individual fish and for interpolation of the P_{AAS-50} , which may prove to be a valuable comparative tool for hypoxic performance both within and across species. Zoologists can now measure the limiting effects of hypoxia in fish that was envisaged by Fry (1947) over 75 years ago.

Acknowledgements

The corresponding author particularly appreciates the numerous insightful discussions with Dr Guy Claireaux and Dr Denis Chabot over the years. We appreciate the logistical assistance from Dr Phillip Morrison and staff in the aquatic facility and workshop at the Department of Zoology, University of British Columbia. We appreciate the constructive feedback provided by two anonymous reviewers.

Competing interests

The authors declare no competing or financial interests.

Author contributions

Conceptualization: Y.Z., A.P.F.; Methodology: Y.Z., D.W.M.; Software: Y.Z.; Validation: Y.Z., D.W.M., C.F.W.; Formal analysis: Y.Z.; Investigation: Y.Z., A.P.F.; Resources: A.P.F.; Data curation: Y.Z., C.F.W.; Writing - original draft: Y.Z.; Writing - review & editing: Y.Z., J.G.R., A.P.F.; Visualization: Y.Z.; Supervision: Y.Z., A.P.F.; Project administration: Y.Z., A.P.F.; Funding acquisition: J.G.R., C.J.B.

Funding

This work was supported by British Columbia Salmon Restoration and Innovation Fund (BCSRIF-083) awarded to J.G.R. and C.J.B. A.P.F. holds a Natural Sciences and Engineering Research Council of Canada Discovery Grant and a Canada Research Chair Tier I. Y.Z. holds a Natural Sciences and Engineering Research Council of Canada Postdoctoral Fellowship.

Data availability

Data are available from figshare: <https://doi.org/10.6084/m9.figshare.19658568.v3>.

References

- Black, C. P. and Tenney, S. M. (1980). Oxygen transport during progressive hypoxia in high-altitude and sea-level waterfowl. *Respir. Physiol.* **39**, 217-239. doi:10.1016/0034-5687(80)90046-8
- Chabot, D. and Claireaux, G. (2008). Environmental hypoxia as a metabolic constraint on fish: the case of Atlantic cod, *Gadus morhua*. *Marine Pollution Bulletin* **57**, 287-294.
- Chabot, D., Steffensen, J. F. and Farrell, A. P. (2016). The determination of standard metabolic rate in fishes. *J. Fish Biol.* **88**, 81-121. doi:10.1111/jfb.12845
- Chabot, D., Zhang, Y. and Farrell, A. P. (2021). Valid oxygen uptake measurements: using high r^2 values with good intentions can bias upward the determination of standard metabolic rate. *J. Fish Biol.* **98**, 1206-1216. doi:10.1111/jfb.14650
- Claireaux, G. and Chabot, D. (2016). Responses by fishes to environmental hypoxia: integration through Fry's concept of aerobic metabolic scope. *J. Fish Biol.* **88**, 232-251. doi:10.1111/jfb.12833
- Claireaux, G. and Lagardère, J.-P. (1999). Influence of temperature, oxygen and salinity on the metabolism of the European sea bass. *J. Sea Res.* **42**, 157-168. doi:10.1016/S1385-1101(99)00019-2
- Claireaux, G., Théron, M., Prineau, M., Dussauze, M., Merlin, F.-X. and Le Floch, S. (2013). Effects of oil exposure and dispersant use upon environmental adaptation performance and fitness in the European sea bass, *Dicentrarchus labrax*. *Aquat. Toxicol.* **130-131**, 160-170. doi:10.1016/j.aquatox.2013.01.004
- Copp, S. W., Davis, R. T., Poole, D. C. and Musch, T. I. (2009). Reproducibility of endurance capacity and $\dot{V}O_2$ peak in male Sprague-Dawley rats. *J. Appl. Physiol.* **106**, 1072-1078. doi:10.1152/jappphysiol.91566.2008
- Douglas, E. L., Friedl, W. A. and Pickwell, G. V. (1976). Fishes in oxygen-minimum zones: blood oxygenation characteristics. *Science* **191**, 957-959. doi:10.1126/science.1251208
- Farrell, A. P., Gamperl, A. K. and Birtwell, I. K. (1998). Prolonged swimming, recovery and repeat swimming performance of mature sockeye salmon *Oncorhynchus nerka* exposed to moderate hypoxia and pentachlorophenol. *J. Exp. Biol.* **201**, 2183-2193. doi:10.1242/jeb.201.14.2183
- Farrell, A. P., Thorarensen, H., Axelsson, M., Crocker, C. E., Gamperl, A. K. and Cech, J. J., Jr (2001). Gut blood flow in fish during exercise and severe hypercapnia. *Comp. Biochem. Physiol. A* **128**, 549-561.
- Fry, F. E. J. (1947). Effects of the environment on animal activity. *Pubis Ont. Fish. Res. Lab.* **68**, 5-62.
- Fry, F. E. J. and Hart, J. S. (1948). The relation of temperature to oxygen consumption in the goldfish. *Biol. Bull.* **94**, 66-77. doi:10.2307/1538211
- Hyman, L. H. (1929). The effect of oxygen tension on oxygen consumption in planaria and some echinoderms. *Physiol. Zool.* **2**, 505-534. doi:10.1086/physzool.2.4.30152973
- Ivy, C. M. and Scott, G. R. (2017). Control of breathing and ventilatory acclimatization to hypoxia in deer mice native to high altitudes. *Acta Physiol.* **221**, 266-282. doi:10.1111/apha.12912
- Jain, K. E., Hamilton, J. C. and Farrell, A. P. (1997). Use of a ramp velocity test to measure critical swimming speed in rainbow trout (*Oncorhynchus mykiss*). *Comp. Biochem. Physiol. A Physiol.* **117**, 441-444. doi:10.1016/S0300-9629(96)00234-4
- Jain, K. E., Birtwell, I. K. and Farrell, A. P. (1998). Repeat swimming performance of mature sockeye salmon following a brief recovery period: a proposed measure of fish health and water quality. *Can. J. Zool.* **76**, 1488-1496. doi:10.1139/z98-079
- Lague, S. L., Chua, B., Alza, L., Scott, G. R., Frappell, P. B., Zhong, Y., Farrell, A. P., McCracken, K. G., Wang, Y. and Milsom, W. K. (2017). Divergent respiratory and cardiovascular responses to hypoxia in bar-headed geese and Andean birds. *J. Exp. Biol.* **220**, 4186-4194. doi:10.1242/jeb.168799
- Lefevre, S., Damsgaard, C., Pascale, D. R., Nilsson, G. E. and Stecyk, J. A. W. (2014). Air breathing in the Arctic: influence of temperature, hypoxia, activity and restricted air access on respiratory physiology of the Alaska blackfish *Dallia pectoralis*. *J. Exp. Biol.* **217**, 4387-4398. doi:10.1242/jeb.105023
- Marras, S., Claireaux, G., McKenzie, D. J. and Nelson, J. A. (2010). Individual variation and repeatability in aerobic and anaerobic swimming performance of European sea bass, *Dicentrarchus labrax*. *J. Exp. Biol.* **213**, 26-32. doi:10.1242/jeb.032136
- Midgley, A. W., McNaughton, L. R. and Carroll, S. (2007). Reproducibility of time at or near $\dot{V}O_{2max}$ during intermittent treadmill running. *Int. J. Sports Med.* **28**, 40-47. doi:10.1055/s-2006-923856
- Mueller, C. A. and Seymour, R. S. (2011). The regulation index: a new method for assessing the relationship between oxygen consumption and environmental oxygen. *Physiol. Biochem. Zool.* **84**, 522-532. doi:10.1086/661953
- Neill, W. H., Miller, J. M., Van Der Veer, H. W. and Winemiller, K. O. (1994). Ecophysiology of marine fish recruitment: a conceptual framework for understanding interannual variability. *Neth. J. Sea Res.* **32**, 135-152. doi:10.1016/0077-7579(94)90037-X
- Prinz, T. S., Zhang, Y., Wegner, N. C. and Dulvy, N. K. (2021). Analytical methods matter too: establishing a framework for estimating maximum metabolic rate for fishes. *Ecol. Evol.* **11**, 9987-10003. doi:10.1002/ece3.7732
- Randall, D. J., Mense, D. and Boutilier, R. G. (1987). The effects of burst swimming on aerobic swimming in chinook salmon (*Oncorhynchus tshawytscha*). *Mar. Behav. Physiol.* **13**, 77-88. doi:10.1080/10236248709378664
- Rummer, J. L. and Brauner, C. J. (2015). Root effect haemoglobins in fish may greatly enhance general oxygen delivery relative to other vertebrates. *PLoS ONE* **10**, e0139477. doi:10.1371/journal.pone.0139477
- Scarabello, M., Wood, C. and Heigenhauser, G. (1991). Glycogen depletion in juvenile rainbow trout as an experimental test of the oxygen debt hypothesis. *Can. J. Zool.* **69**, 2562-2568. doi:10.1139/z91-361
- Scarabello, M., Heigenhauser, G. J. and Wood, C. M. (1992). Gas exchange, metabolite status and excess post-exercise oxygen consumption after repetitive bouts of exhaustive exercise in juvenile rainbow trout. *J. Exp. Biol.* **167**, 155-169. doi:10.1242/jeb.167.1.155
- Seibel, B. A., Andres, A., Birk, M. A., Burns, A. L., Shaw, C. T., Timpe, A. W. and Welsh, C. J. (2021). Oxygen supply capacity breathes new life into critical oxygen partial pressure (P_{crit}). *J. Exp. Biol.* **224**, jeb242210. doi:10.1242/jeb.242210
- Steinhausen, M. F., Sandblom, E., Eliason, E. J., Verhille, C. and Farrell, A. P. (2008). The effect of acute temperature increases on the cardiorespiratory performance of resting and swimming sockeye salmon (*Oncorhynchus nerka*). *J. Exp. Biol.* **211**, 3915-3926. doi:10.1242/jeb.019281
- Tang, P.-S. (1933). On the rate of oxygen consumption by tissues and lower organisms as a function of oxygen tension. *Q. Rev. Biol.* **8**, 260-274. doi:10.1086/394439
- Terrados, N., Melichna, J., Sylvén, C., Jansson, E. and Kaijser, L. (1988). Effects of training at simulated altitude on performance and muscle metabolic capacity in competitive road cyclists. *Eur. J. Appl. Physiol. Occup. Physiol.* **57**, 203-209. doi:10.1007/BF00640664
- Uitsch, G. R., Ott, M. E. and Heisler, N. (1980). Standard metabolic rate, critical oxygen tension, and aerobic scope for spontaneous activity of trout (*Salmo gairdneri*) and carp (*Cyprinus carpio*) in acidified water. *Comp. Biochem. Physiol. A Physiol.* **67**, 329-335. doi:10.1016/S0300-9629(80)80004-1

- Wagner, G. N., Kuchel, L. J., Lotto, A., Patterson, D. A., Shrimpton, J. M., Hinch, S. G. and Farrell, A. P.** (2006). Routine and active metabolic rates of migrating adult wild sockeye salmon (*Oncorhynchus nerka* Walbaum) in seawater and freshwater. *Physiol. Biochem. Zool.* **79**, 100-108. doi:10.1086/498186
- Warburg, O.** (1914). Beiträge zur Physiologie der Zelle, insbesondere über die Oxydationsgeschwindigkeit in Zellen. *Ergeb. Physiol.* **14**, 253-337. doi:10.1007/BF02188636
- Weber, R. E., Jensen, F. B. and Cox, R. P.** (1987). Analysis of teleost hemoglobin by Adair and Monod-Wyman-Changeux models. *J. Comp. Physiol. B* **157**, 145-152. doi:10.1007/BF00692358
- Wood, C. M.** (1991). Acid-Base and ion balance, metabolism, and their interactions, after exhaustive exercise in fish. *J. Exp. Biol.* **160**, 285-308. doi:10.1242/jeb.160.1.285
- Zhang, Y.** (2021). Interpreting species, intraspecific and intra-individual variability by comprehensively characterizing a fish's respiratory phenotype with valid measures of oxygen uptake. *PhD thesis*, University of British Columbia. doi:10.14288/1.0396683
- Zhang, Y. and Gilbert, M. J. H.** (2017). Comment on 'Measurement and relevance of maximum metabolic rate in fishes by Norin & Clark (2016)'. *J. Fish Biol.* **91**, 397-402. doi:10.1111/jfb.13291
- Zhang, Y., Claireaux, G., Takle, H., Jørgensen, S. M. and Farrell, A. P.** (2018). A three-phase excess post-exercise oxygen consumption in Atlantic salmon *Salmo salar* and its response to exercise training. *J. Fish Biol.* **92**, 1385-1403. doi:10.1111/jfb.13593
- Zhang, Y., Gilbert, M. J. H. and Farrell, A. P.** (2019). Finding the peak of dynamic oxygen uptake during fatiguing exercise in fish. *J. Exp. Biol.* **222**, jeb196568. doi:10.1242/jeb.196568
- Zhang, Y., Gilbert, M. J. H. and Farrell, A. P.** (2020). Measuring maximum oxygen uptake with an incremental swimming test and by chasing rainbow trout to exhaustion inside a respirometry chamber yields the same results. *J. Fish Biol.* **97**, 28-38. doi:10.1111/jfb.14311
- Zhang, Y., So, B. E. and Farrell, A. P.** (2021). Hypoxia performance curve: assess a whole-organism metabolic shift from a maximum aerobic capacity towards a glycolytic capacity in fish. *Metabolites* **11**, 447. doi:10.3390/metabo11070447

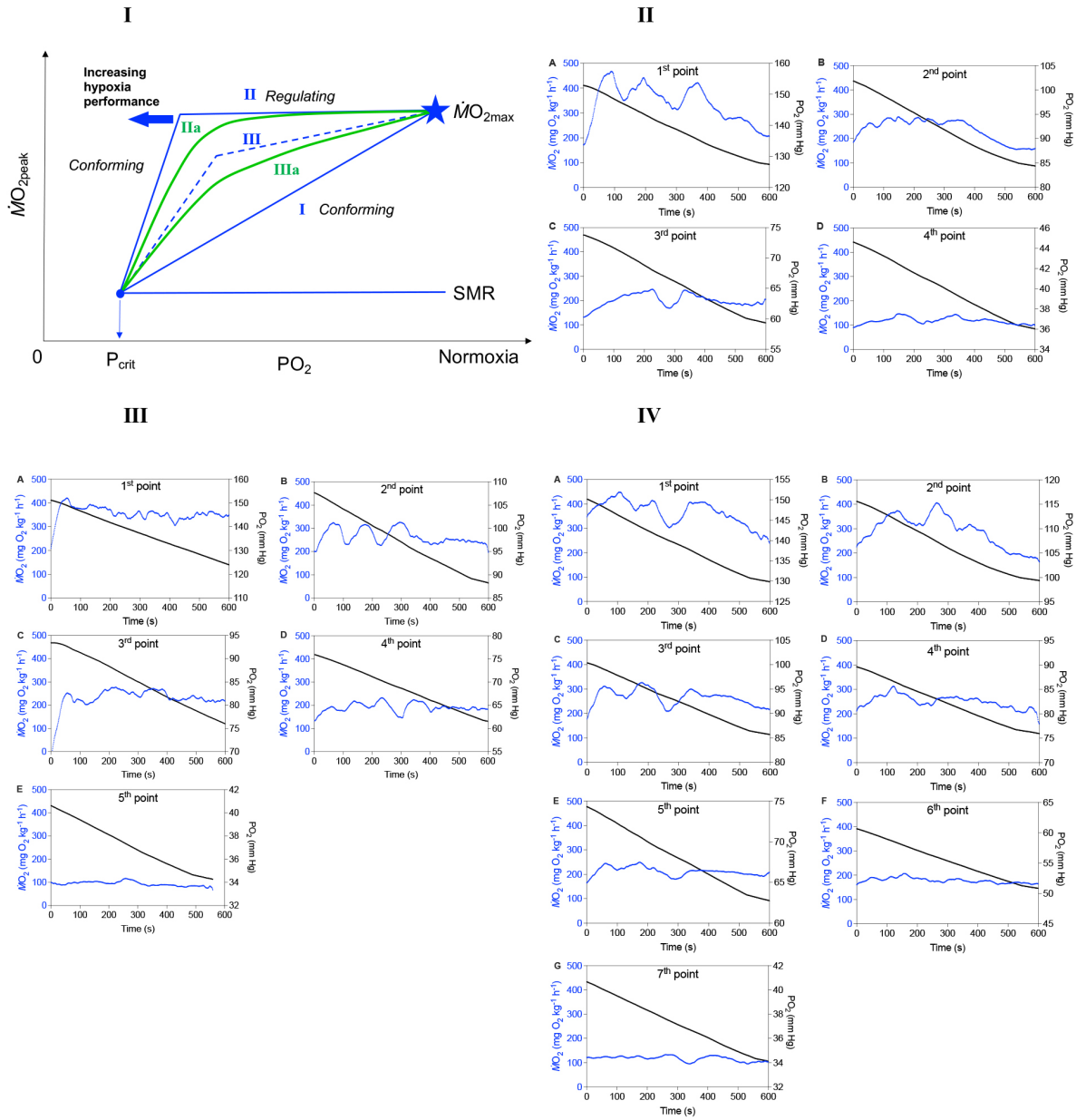


Fig. S1. The detailed elucidation of hypoxic performance models (section I). Model I represent a scenario when a fish regulates $\dot{M}O_{2\text{peak}}$ at $\dot{M}O_{2\text{max}}$ until a threshold PO_2 is reached, below which $\dot{M}O_{2\text{peak}}$ declines linearly to converge with $\dot{M}O_{2\text{min}}$ at a critical PO_2 (P_{crit}). Model Ia is a variation on Model I where the transition from the regulating to the conforming states is more gradual. Model II represents a linear conformity of $\dot{M}O_{2\text{peak}}$ with ambient PO_2 . Model III presents two different phases of linear conformity with ambient PO_2 where $\dot{M}O_{2\text{peak}} < \dot{M}O_{2\text{max}}$ except in normoxia and a threshold PO_2 exists. Model IIIa represents a curvilinear relationship between $\dot{M}O_{2\text{peak}}$ between normoxia and P_{crit} , which is a variation on Model III but one where conformation with ambient increases progressively rather than abruptly with ambient PO_2 . To demonstrate the measurements of each point used for model hypoxic performance curve, we showed the representative examples of off-line, continuous analysis of oxygen uptake ($\dot{M}O_2$, blue lines) for an individual rainbow trout (*Oncorhynchus mykiss*) during a 300-s chase inside a respirometer and during the ensuing 300-s recovery period (section II: 4-point model, section III: 5-point model, section IV: 7-point model). Panel A in each section shows the chase in normoxia and the other panels in the same section show the progressively lower ambient dissolved water oxygen levels for the same fish to illustrate that peak oxygen uptake ($\dot{M}O_{2\text{peak}}$) can be reached multiple times during the chase and sometimes, but not always, immediately after the chase and that is constrained by progressive hypoxia. All $\dot{M}O_{2\text{peak}}$ values were determined on individual fish using an iterative algorithm that coupled a rolling regression analysis and a reliable minimum duration for the sampling window (100 s, see analysis in Fig. S2). Since the respirometer remained closed for the entire 600-s recording period, the corresponding decline in the dissolved oxygen level (black lines) that was used to calculate $\dot{M}O_2$ is also shown on the same time axis.

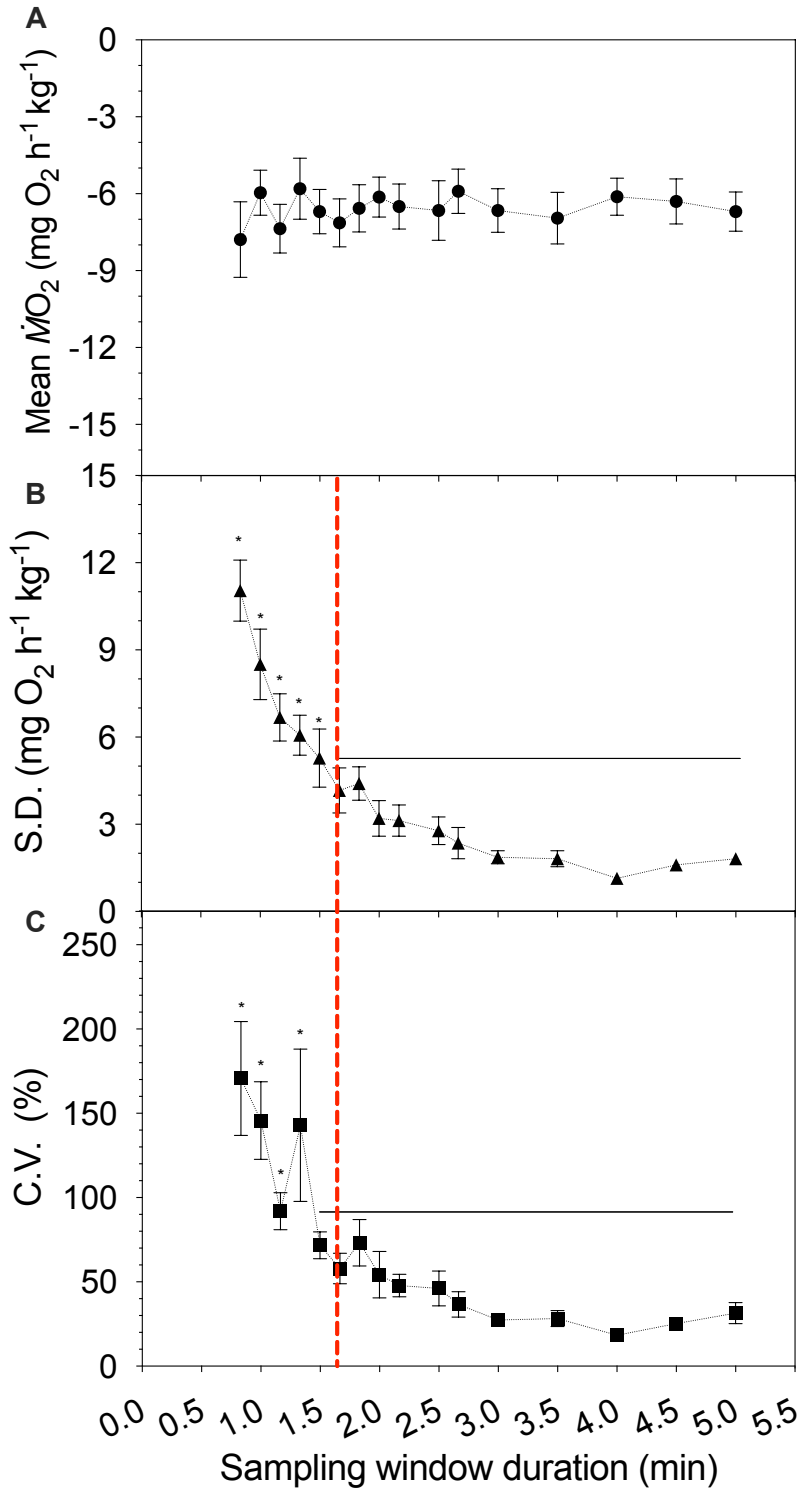


Fig. S2. An analysis of the impact of varying the duration of the sampling window when making an estimate of the rate of oxygen uptake ($\dot{M}O_2$). Traces for constant background $\dot{M}O_2$ (A) of an empty respirometer at 16 °C (20-min in total duration; n=8) were used to analyze the signal ($\dot{M}O_2$)-to-noise (statistical variation) ratio. Both (B) standard deviation (S.D.) and (C) coefficient of variation (C.V.) used as estimates of the statistical variation (noise associated with a constant $\dot{M}O_2$ signal) by compiling mean $\dot{M}O_2$ and its statistics from the eight $\dot{M}O_2$ traces as a function of sampling window duration. The S.D. and C.V. values for each sampling window duration were compared using a one-way ANOVA with Tukey's *post-hoc* tests ($\alpha < 0.05$). All values are presented as mean \pm s.e.m.. The criterion for selecting minimum duration for the sampling window was the duration prior to a statistical increase in either the S.D. or C.V. of the mean $\dot{M}O_2$ which did not necessarily change from a stable value with longer sampling window durations. This minimum duration proved to be 100 s (vertical red dashed line) although a numerical increase in the mean value seemed to begin with a sampling window duration of <180 s.

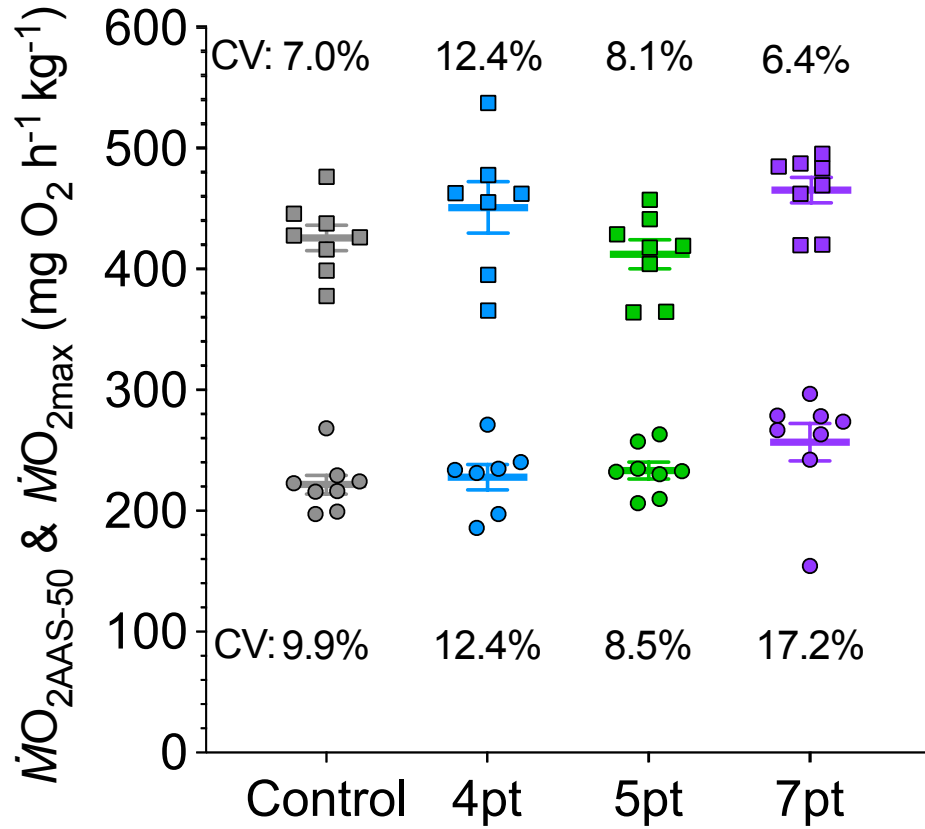


Fig. S3. A comparison of mean (\pm s.e.m.) peak oxygen uptake at the 50% of absolute aerobic scope ($\dot{M}O_{2AAS-50}$) and mean maximum oxygen uptake ($\dot{M}O_{2max}$) among the three different experimental designs: four-point (4 pt), five-point (5 pt) and seven-point (7 pt) levels of progressive hypoxia. There was not statistical significance (one-way ANOVA Holm-Šídák's *post-hoc* tests). Coefficient of variation (CV) for these mean values are given and the individual values for $\dot{M}O_{2AAS-50}$ (circles) and $\dot{M}O_{2max}$ (squares) for each test group are also shown.